Compound buckling-swelling mechanism of the earth surface folding: FE modeling study related to the Pannonian Basin

Marek Jarosiński
Polish Geological Institute, *marek.jarosinski@pgi.gov.pl*

Introduction

The aim of the modeling study was to check the stress and strain distribution within intra-continental lithosphere during neotectonic phase of compression using rheological layering of the lithosphere model as much realistic as possible. Finite element 2D model was constructed along the Cel05 deep seismic sounding line (Grad et al., 2006) passing through: East European Craton (EEC), Carpathians and Pannonian Basin (PB) and was extended southwestwards across the Dinarides. The section is 1200 km long and 250 km deep, reaching asthenosphere. There are large contrasts in lithospheric strength across the section from an extremely warm, thin and weak Pannonian Basin through the transitional Dinarides and Carpathians towards a thick, cold and strong East European Craton (Jarosiński & Dąbrowski, 2002). The trend of the line is similar to the recent and neotectonic maximum horizontal stress direction (Gerner, 1999; Jarosiński, 2005) which allows modeling contraction in a plain strain conditions. In this approach we were not able to simulate strike-slip deformation which obviously also played a role in neotectonic deformation of the Pannonian Basin (Fodor et al., 2005) besides the typical inversion structures controlled by thrust fault stress regime. Bearing above in mind, we do not intend to replicate the real neotectonic structures of the Pannonian Basin but rather to check a realistic scale and pattern of basin inversion structures and also assess evolution of lithosphere mechanics during contraction inversion.

Rheology of rock materials

Coupled elastoviscoplastic material behavior is assumed for each layer in the model, including Von Mises failure criteria for plastic strain (artificially coupled with temperature - Jarosiński et al., in press) and power law creep for viscous strain.

Lithological layering of the lithosphere was determined from seismic wave velocity model based on seismic refraction model. Each layer is assumed to comprise a mixture of rocks typical for given lithospheric strata and characterized by an average P wave velocity adjusted to the seismic model (based on Christensen & Mooney, 1995). Parameters of power law creep function for each layer were calculated as a mean for lithological components taking into account wet and dry rheology. Arithmetic and geometric means were calculated for representative parameters, according to procedure given by Ji & Xia (2002) for constant stress and constant strain rate cases. Asthenosphere were simulated by lithosphere mantle material with decreased viscosity by increasing pre-exponent factor in power-law creep function by one order of magnitude. Artificially high heat conductivity was implemented to asthenosphere in order to simulate heat transfer by convection. Finally, 9 types of lithospheric layers were distinguished in this model: sedimentary or metamorphic (SED/MET), weak and strong upper crust (UCa, UCb), middle crust (MC), weak and strong lower crust (LCa, LCb), weak and strong lithospheric mantle (UMa, UMb) and the asthenosphere (AST). Density was coupled with temperature by expansion coefficient λ = 3e-5 /°K.

Model set up and modeling procedure

Precise model discretization was used with the nominal size of the triangular elements in the crust, mantle and asthenosphere: 2, 4 and 8 km, respectively. This model comprise over 200 000 degrees of freedom. Kinematic boundary conditions correspond to neotectonic stage of compression in the Pannonian region. A push from the Adriatic side was applied with an overall horizontal strain rate 10^{-16} s^{-1} through 7.5 Ma. The finite element model was solved using ANSYS 10 code, deforming Lagrangian 2D mesh with SOLID82 triangular plane stain elements. Due to a minor finite strain (less then 3%), temperature was not recalculated and also mass transfer and heat generation by mechanical strain were neglected.

Each modeling run was performed in several steps: (1) Thermal modeling with standard boundary conditions and radiogenic heat production adjusted by trial and error procedure until a good fit to surface heat flux was obtained. (2) Model loading by gravity and temperature simultaneously. (3) Model relaxation until isosatic equilibrium was achieved. (4) Tectonic, kinematic loading with constant velocity at the SW model boundary. Nodes displacement on each step of analyses was normalized to nodes position in isostatically balanced model, after the third step of loading.

Modeling results

Results of modeling show evolution of stress regime before and during basin inversion. After beginning of tectonic contraction in the Pannonian Basin thrust fault stress regime was established almost instantaneously in the UM and LC whilst strike–slip stress regime persists in the UC until 1-1.5 Ma of contraction. After 2-2.5 Ma of contraction elastic cores of the strongest lithospheric layers vanished in the basin and steady state stress conditions emerged.

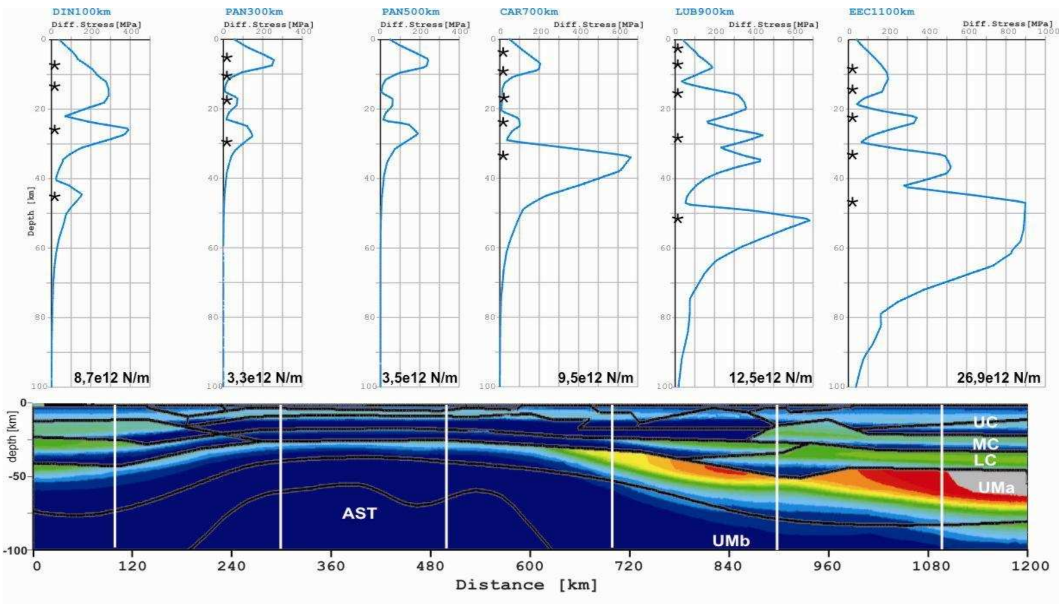

Fig. 1 – Results of differential stress modeling after 5 Ma of contraction (steady state stress conditions). Diagrams show 2D strength envelopes for locations marked at the model below: Dinarides, 2 profiles for Pannonian Basin, Carpathians, Lublin Basin and EEC.

Deformation pattern reveals complex mechanism of earth surface (Topo) folding. After 1 Ma of contraction three regular, first-order buckling folds raised within the lithosphere (Dinaric, intrabasin and Carpathian folds) with an amplitude of 400 m and wavelength of c.a. 180 km. The Dinaric and Carpathian folds formed in position characteristic for marginal bulges within transition zone from the thin basin-type lithosphere to the thick flank-type one (Jarosiński et al., in press). The rate of folds growth decreases parallel with vanishing elastic cores of strong layers, thus after 2 Ma of contraction folds amplitude reaches 550 m. At the same time, the second-order, short wavelength (50 km) fold generation appears in result of detached UC buckling driven by thrust fault stress regime.

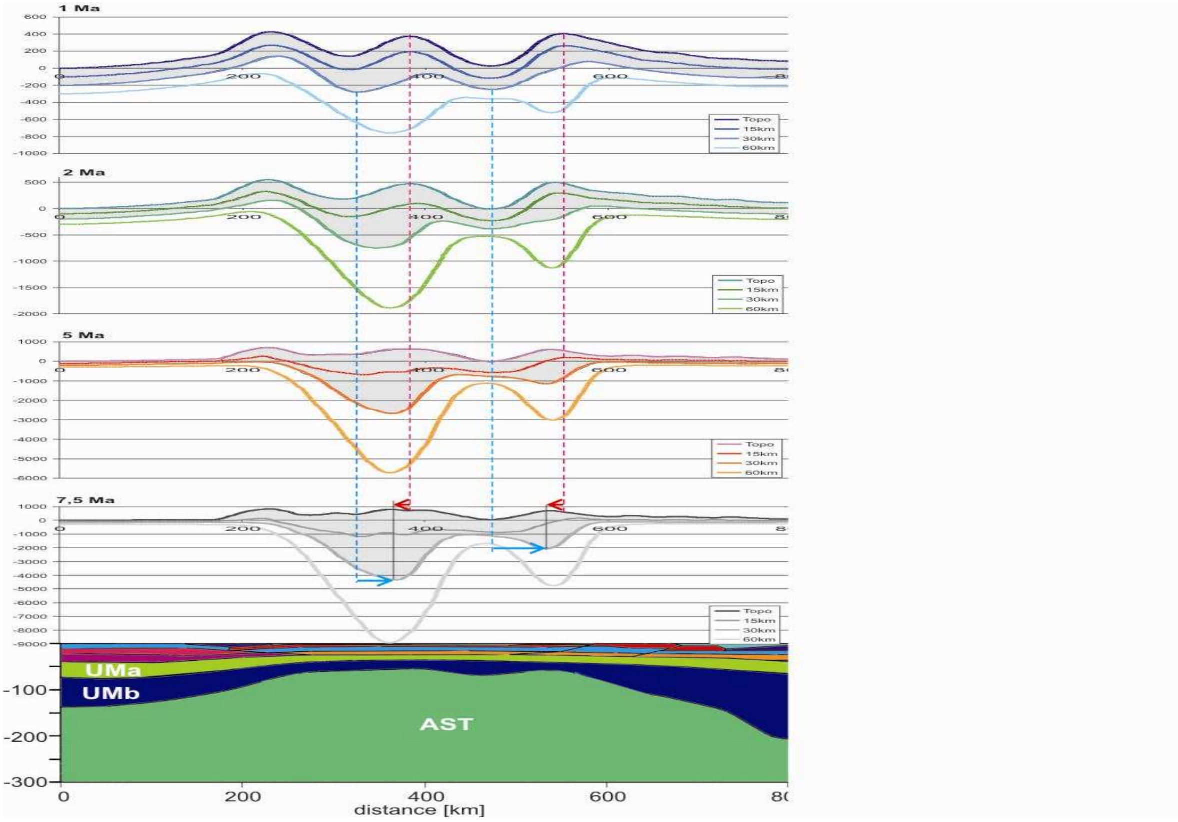

Fig. 2 – Evolution of the Topo surface folding in the Pannonian Basin segment of the model. Diagrams represent deformation after 1, 2, 5 and 7.5 Ma of shortening. Each diagram shows folding of horizontal lines which represent Topo surface and the bottom of UC, LC and lithosphere within the basin. Sequence of diagrams illustrate transition from buckling to swelling mechanism of folding and migration of the folds' hinges indicated by dashed lines and arrows.

Further contraction of the lithosphere lacking elastic cores of strong layers causes faster tectonic contraction of hot and rheologically weakest segments of the basin (Fig. 2).. In result crust of these segments becomes thicker and causes the Topo to be uplifted due to isostatic compensation. This causes lateral migration of the anticlines at the Topo and synclines at the Moho towards the weakest segments of the basin and, after 7.5 Ma of contraction, creates characteristic swell-like pattern in the crust. Compound, buckling-swelling mechanism of folding lead to 800 m high anticlines at the Topo surface. This mechanism of Topo folding is significantly more effective than simple buckling mechanism of an elastic plate presented by Horváth & Cloetingh (1996) who were able to produce maximum 200 m high anticlines in similar shortening conditions.

Taking into account a density contrast across the Moho, it was estimated that the anticlines are only partially supported by crustal roots. For Dinaric, intra-basin and

Carpathian anticlines, respectively, only 10%, 65% and 35% of their elevation are isostatically balanced. This indicates individual complex buckling-swelling origin of each anticline. In general, buckling plays a dominant role in the beginning of contraction when elastic cores of the strong lithospheric layers are present. Swelling combined with isostatic rebound becomes more effective in later stage of inversion, when a steady state viscoplastic strain takes over elastic buckling in the weakest segments of the model.

References

Christensen, N.I. and W.D. Mooney, 1995, Seismic velocity structure and composition of the continental crust: A global view, J. Geophys. Res., 100, 9761-9788.

Horváth, F., Cloetingh, S. 1996: Stress-induced late-stage subsidence anomalies in the Pannonian basin. Tectonophysics 266, pp. 287–300.

Fodor, L., Bada, G., Csillag, G., Horvath, E., Ruszkiczay-Rüdiger, Z., Palotás, K., Síkhegyi, F., Timár, G., Cloetingh, S., Horvath, F., 2005. An outline of neotectonic structures and morphotectonics of the western and central Pannonian Basin. Tectonophysics 410, 15-41.

Gerner, P., Bada, G., Dövenyi, P., Müller, B., Oncescu, M., Cloetingh S., Horvath F., 1999, Recent tectonic stress and crustal deformation in and around the Pannonian Basin: data and models. In: The Mediterranean Basins: Tertiary Extension within the Alpine Orogen, eds. Durand, B., Jolivet, L., Horvath F., & Seranne, M., Geol. Soc, Lond. Spec. Publ. 156, 269–294.

Grad M., Guterch A., Keller G. R., Janik T., Hegedűs E., Vozár J., Ślączka A., Tiira T., Yliniemi J., 2006. Lithospheric structure beneath trans-Carpathian transect from Precambrian platform to Pannonian basin: CELEBRATION 2000 seismic profile CEL05. J. Geophys. Res. 111, B03301, doi:10.1029/2005JB003647Jarosiński & Dąbrowski, 2002

Jarosinski, M., 2005. Ongoing tectonic reactivation of the Outer Carpathians and its impact on the foreland: Results of borehole breakout measurements in Poland. Tectonophysics 410, 189-216Jarosinski, M., Beekman, F., Matenco L., Cloetingh, S., 2010. Mechanics of basin inversion: finite element modelling of the Pannonian Basin System. Tectonophysics, in press.

Jarosiński M., Dąbrowski M., 2006. Rheological models of the lithosphere arcross the Trans-European Suture Zone in northern and western part of Poland (in Polish with English summary). Prace PIG, 188: 143-166.

Ji, S., Xia, B., 2002. Rheology of Polyphase Earth Materials. Polytechnic International Press, Montreal, 259.